Metabolic balance of coastal Antarctic waters revealed by autonomous pCO_2 and $\Delta O_2/Ar$ measurements

Citation	Tortell, P. D., Asher, E. C., Ducklow, H. W., Goldman, J. A. L., Dacey, J. W. H., Grzymski, J. J., Young, J. N., Kranz, S. A., Bernard, K. S., & Morel, F. M. M. (2014). Metabolic balance of coastal Antarctic waters revealed by autonomous pCO_2 and $\Delta O_2/Ar$ measurements. Geophysical Research Letters, 41(19), 6803–6810. doi:10.1002/2014GL061266
DOI	10.1002/2014GL061266
Publisher	American Geophysical Union
Version	Version of Record
Terms of Use	http://cdss.library.oregonstate.edu/sa-termsofuse

AGU PUBLICATIONS

Geophysical Research Letters

RESEARCH LETTER
10.1002/2014GL061266

Key Points:
- Metabolic balance of Antarctic waters is highly dynamic over various time scales
- Autonomous methods can capture biological variability
- Light availability and grazing control summer time net community production

Supporting Information:
- Readme
- Figures S1–S3

Correspondence to:
P. D. Tortell,
ptortell@eos.ubc.ca

Citation:
Tortell, P. D., E. C. Asher, H. W. Ducklow, J. A. L. Goldman, J. W. H. Dacey, J. J. Grzymski, J. N. Young, S. A. Kranz, K. S. Bernard, and F. M. M. Morel (2014), Metabolic balance of coastal Antarctic waters revealed by autonomous pCO_2 and ΔO_2/Ar measurements, *Geophys. Res. Lett.*, *41*, 6803–6810, doi:10.1002/2014GL061266.

Received 18 JUL 2014
Accepted 21 JUL 2014
Accepted article online 4 AUG 2014
Published online 3 OCT 2014

Metabolic balance of coastal Antarctic waters revealed by autonomous pCO_2 and ΔO_2/Ar measurements

Philippe D. Tortell[1,2], Elizabeth C. Asher[1], Hugh W. Ducklow[3], Johanna A. L. Goldman[4], John W. H. Dacey[5], Joseph J. Grzymski[6], Jodi N. Young[4], Sven A. Kranz[4], Kim S. Bernard[7], and François M. M. Morel[4]

[1]Department of Earth, Ocean and Atmospheric Sciences, University of British Columbia, Vancouver, British Columbia, Canada, [2]Department of Botany, University of British Columbia, Vancouver, British Columbia, Canada, [3]Lamont Doherty Earth Observatory, Columbia University, Palisades, New York, USA, [4]Department of Geosciences, Princeton University, Princeton, New Jersey, USA, [5]Biology Department, Woods Hole Oceanographic Institution, Woods Hole, Massachusetts, USA, [6]Division of Earth and Ecosystem Sciences, Desert Research Institute, Reno, Nevada, USA, [7]College of Earth, Ocean, and Atmospheric Sciences, Oregon State University, Corvallis, Oregon, USA

Abstract We use autonomous gas measurements to examine the metabolic balance (photosynthesis minus respiration) of coastal Antarctic waters during the spring/summer growth season. Our observations capture the development of a massive phytoplankton bloom and reveal striking variability in pCO_2 and biological oxygen saturation (ΔO_2/Ar) resulting from large shifts in community metabolism on time scales ranging from hours to weeks. Diel oscillations in surface gases are used to derive a high-resolution time series of net community production (NCP) that is consistent with ^{14}C-based primary productivity estimates and with the observed seasonal evolution of phytoplankton biomass. A combination of physical mixing, grazing, and light availability appears to drive variability in coastal Antarctic NCP, leading to strong shifts between net autotrophy and heterotrophy on various time scales. Our approach provides insight into the metabolic responses of polar ocean ecosystems to environmental forcing and could be employed to autonomously detect climate-dependent changes in marine primary productivity.

1. Introduction

The metabolic balance of an ecosystem, defined as gross photosynthesis minus community respiration (i.e., net community production; NCP), governs its potential for biomass accumulation and carbon storage [*Ducklow and Doney*, 2013]. Highly productive polar and subpolar marine waters exhibit a strong seasonal decoupling between photosynthesis and respiration, leading to the accumulation and subsequent loss of organic carbon from the surface mixed layer [*Smith et al.*, 2011; *Sweeney et al.*, 2000]. Accurate and routine determination of NCP in these regions is constrained by a number of methodological and logistical factors. In vitro incubations capture short-term rates of photosynthesis and respiration, but they are subject to sample containment artifacts [*Quay et al.*, 2010; *Williams et al.*, 2013] and difficult to extrapolate to ecologically relevant scales [*Williams et al.*, 2013]. Conversely, discrete in situ geochemical tracer measurements provide temporally and spatially integrated NCP estimates [*Emerson et al.*, 1995; *Reuer et al.*, 2007] but do not resolve short-term productivity responses to rapid environmental fluctuations that are characteristic of polar systems. Here we use high-frequency, continuous measurements of surface water pCO_2 and biological O_2 saturation (ΔO_2/Ar) to examine the in situ metabolic balance of coastal Antarctic waters adjacent to the Palmer Station Long Term Ecological Research site (PAL-LTER).

Time series observations at PAL-LTER have provided information on the seasonal and interannual variability of photosynthesis and bacterial production in near-shore waters of the West Antarctic Peninsula (WAP) [*Ducklow*, 2008; *Moline and Prezelin*, 1996; *Ducklow et al.*, 2007; *Smith et al.*, 1998]. Remote sensing has revealed large climate-driven changes in surface water phytoplankton distributions over the past two decades [*Montes-Hugo et al.*, 2009], while ship-based measurements along the WAP have provided information on interannual and regional NCP variability [*Carrillo et al.*, 2004; *Huang et al.*, 2012]. While satellite observations are often limited by cloud cover and do not directly quantify the in situ metabolic balance, field observations in the WAP have focused on a relatively small portion of the phytoplankton growing season and thus do not fully resolve

seasonal cycles. By comparison, our time series observations capture the seasonal dynamics of surface water NCP in coastal WAP waters with unprecedented resolution, demonstrating ecosystem metabolic responses to physical and biological forcing over a range of time scales.

2. Methods

Dissolved gases were measured using membrane inlet mass spectrometry (MIMS), [*Tortell*, 2005] in seawater from the unfiltered seawater pump supply (SWP) drawn from 6 m depth in Arthur Harbor, adjacent to the PAL-LTER laboratories (Figure S1 in the supporting information). Temperature-controlled seawater standards were used to calibrate pCO_2 and biological O_2 saturation ($\Delta O_2/Ar$) measurements [*Tortell et al.*, 2011]. $\Delta O_2/Ar$ represents the percent deviation in the seawater O_2/Ar ratio from air equilibrium, with Ar normalization used to remove physical (e.g., temperature dependent) effects on O_2 saturation state [*Craig and Hayward*, 1987]. We used a simple mass balance approach to derive estimates of NCP from daily mixed layer changes in $\Delta O_2/Ar$ [*Kaiser et al.*, 2005]. In the absence of strong lateral and vertical inputs (discussed below), the change in mixed layer $\Delta O_2/Ar$ represents the combined effects of NCP (J_{bio}) and sea-air gas exchange (J_{ex}).

$$dO_2/Ar/dt = J_{bio} + J_{ex} \quad (1)$$

Using a 1 h averaging time step, we computed the rate of change in surface $\Delta O_2/Ar$ (i.e., $[\Delta O_2/Ar_t - \Delta O_2/Ar_{t-1}]/\Delta t$), and the associated sea-air flux term using a wind speed dependent gas exchange coefficient [*Wanninkhof*, 1992]. Hourly rates of NCP were derived from the observed change in $\Delta O_2/Ar$, corrected for sea-air flux, and integrated over a 24 h period to obtain daily NCP estimates (mmol O_2 m^{-3} d^{-1}). NCP was converted into C units assuming a photosynthetic quotient of 1.0, derived from an analysis of diel changes in O_2 and dissolved inorganic carbon (DIC) concentrations (described below) during each daily cycle.

Additional measurements were collected in semiweekly samples at PAL-LTER Station B (Figure S1), located 1 km from the SWP intake. Depth profiles of temperature and salinity were obtained using a Seabird SBE 19*plus* SeaCAT Profiler, while macronutrient and chlorophyll a (Chl *a*) concentrations (used as a metric of total phytoplankton biomass) were measured in 10 m depth seawater samples following standard Joint Global Ocean Flux Study protocols [*Knap et al.*, 1996]. Total alkalinity was measured via potentiometric titration of $HgCl_2$-preserved samples [*Brewer et al.*, 1986], calibrated against certified standards (supplied by Dr. Andrew Dickson, Scripps Institution of Oceanography). Dissolved inorganic carbon was computed from measured pCO_2 and alkalinity using CO2SYS [*Pierrot et al.*, 2006] with the equilibrium constants of *Mehrbach et al.* [1973] refit by *Dickson and Millero*, [1987].

Measurements of the maximum quantum yield of Photosystem II (PSII) charge separation (F_v/F_m) were performed using an in situ Fluorescence Induction and Relaxation system (FiRe, Satlantic) following published methodologies [*Gorbunov et al.*, 1999]. The instrument was connected in flow-through mode to the SWP in parallel with the MIMS sampling line. Net primary production was measured in ~10 m depth seawater samples from Station B using 24 h ^{14}C incubations [*Knap et al.*, 1996]. Incubation bottles for productivity measurements were held in an outdoor flow-through incubator with one layer of neutral density screening (~50% of surface irradiance). Surface PAR levels (i.e., photosynthetically active radiation; 400–700 nm wavelength) and wind speed data were obtained from the meteorological sensors on top of the Palmer Station Terra Laboratory.

Krill abundances were determined between December and February using acoustic surveys [*Bernard and Steinberg*, 2013] along a standard set of transects around Palmer Station. Daily krill grazing rates (mg Chl *a* m^{-2} d^{-1}) were estimated as the product of depth-integrated abundances and a mean specific ingestion rate (3.6 μg Chl *a* $ind.^{-1}$ d^{-1} [*Bernard et al.*, 2012]). Additional measurements of microzooplankton grazing rates were obtained from five dilution experiments [*Landry et al.*, 1995] conducted over the course of the sampling season.

3. Results and Discussion

3.1. Seasonal Cycle of Phytoplankton Biomass, Hydrography, and Nutrients

The 2012/2013 growth season was characterized by a massive spring phytoplankton bloom in the waters adjacent to Palmer Station (Figure 1a). This bloom developed in response to mixed layer stratification (Figures 1c and 1d) and reached peak Chl *a* concentrations (>40 mg m^{-3}) that were among the highest ever

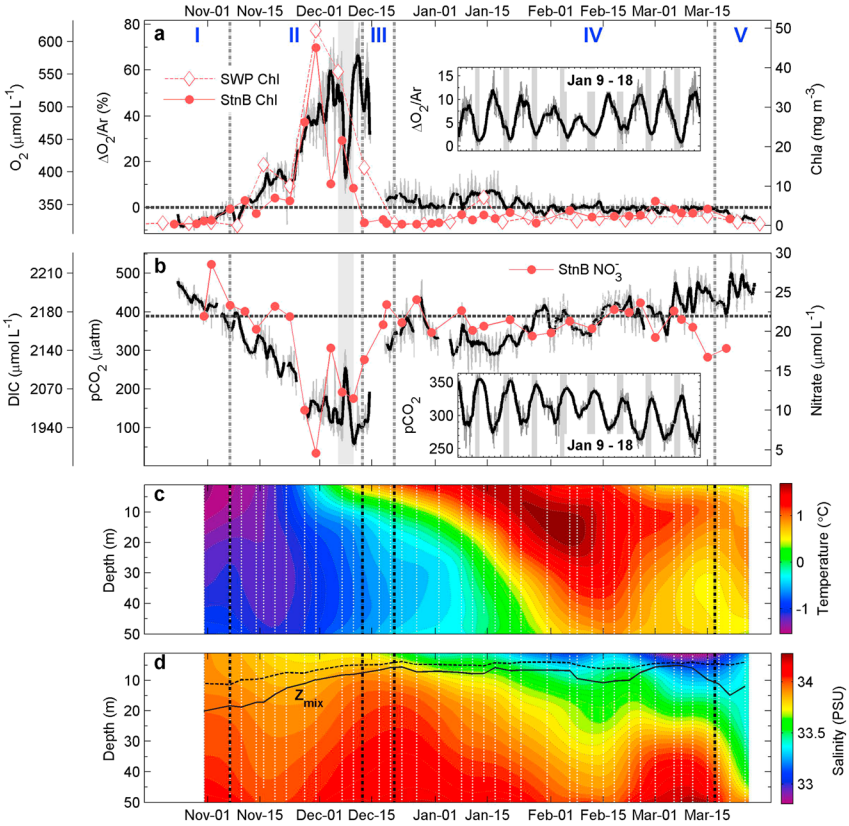

Figure 1. Time series of (a) $\Delta O_2/Ar$, chlorophyll, (b) pCO_2, nitrate, (c) temperature, and (d) salinity during the 2012–2013 spring/summer season at Palmer Station. SWP denotes the Arthur Harbor seawater intake supply, while Stn B denotes PAL-LTER Station B. Inset figures show diel $\Delta O_2/Ar$ and pCO_2 cycles in mid-January, with grey patches denoting night time. Vertical lines and roman numerals indicate phases of the seasonal cycle, while horizontal lines in Figures 1a and 1b indicate atmospheric equilibrium values for DO_2/Ar and pCO_2, respectively. The grey patches in Figures 1a and 1b highlight a short-lived pCO_2 and $\Delta O_2/Ar$ excursion in early December. Z_{mix} in Figure 1d represents the computed mixed layer ($\Delta\sigma_t$ of 0.125 kg m^{-3}) at Station B.

recorded in the ~20 year PAL-LTER archive (http://oceaninformatics.ucsd.edu/datazoo/data/pallter/datasets). Peak Chl *a* concentrations measured in the SWP were similar to those in discrete samples collected at Station B (Figure 1a), suggesting that Arthur Harbor was broadly representative of the near-shore environment surrounding Palmer Station. Following the strong increase in Chl *a* concentrations, the phytoplankton bloom crashed over a 2 week period in early December, rapidly declining to prebloom values. Phytoplankton biomass remained relatively low for the rest of the sampling season, with only a small secondary bloom (~6 mg Chl *a* m^{-3}) observed in early March.

The accumulation of phytoplankton biomass led to significant nutrient drawdown (minimum NO_3^- concentrations of ~5 µmol L^{-1}; Figure 1b). Conversely, the crash of the phytoplankton bloom was associated with a sharp increase in surface NO_3^- concentrations, indicative of a physical entrainment process. Indeed, conductivity-temperature-depth profile data from Station B showed a pronounced upward doming of isohalines in early/mid-December (Figure 1d), coincident with the increased surface water NO_3^- and decreased Chl *a*. A smaller, transient increase in NO_3^- was also observed prior to the bloom crash. These high-salinity intrusions suggest mixing of high NO_3^-/low Chl *a* deep waters into the surface layer, associated with the transport of warm, nutrient-rich Upper Circumpolar Deep Water onto the continental shelf. Our observations thus suggest that physical mixing played a significant role in diluting phytoplankton biomass during the crash of the spring bloom, as observed in previous studies [*Prezelin et al.*, 2004].

The persistence of low summer Chl *a* despite high nutrient levels and strong mixed layer stratification is not likely attributable to iron limitation, which is widespread across the pelagic Southern Ocean [*Boyd*, 2002]. Active Chl *a* fluorescence measurements from the SWP supply suggest that the phytoplankton

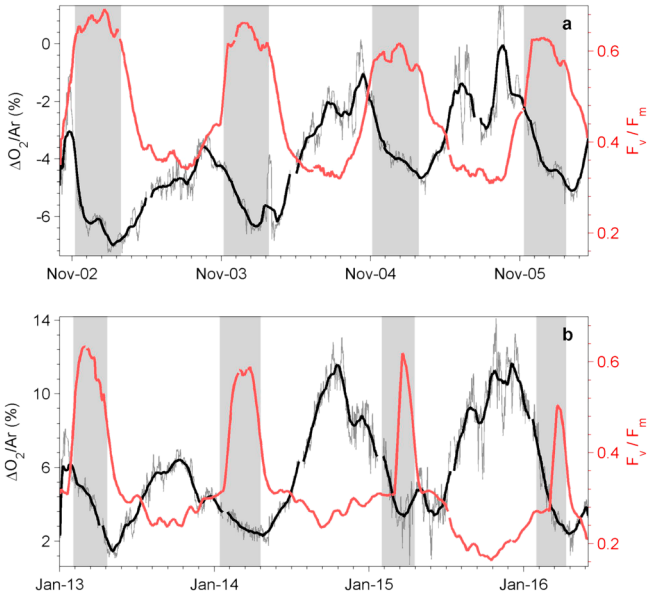

Figure 2. Time series of $\Delta O_2/Ar$ and photochemical quantum efficiency of Photosystem II (F_v/F_m) over four consecutive diel cycles in the (a) early and (b) midseason growth periods. Grey bars represent nighttime.

assemblages were iron replete, with high photosynthetic quantum efficiencies ($F_v/F_m \sim 0.55$) observed over the entire summer growth period. In the absence of nutrient limitation, the net accumulation of midsummer phytoplankton biomass was likely controlled by zooplankton grazing. Based on our measurements of potential krill and microzooplankton grazing rates, we estimate grazing losses ranging from ~10 to 100 mg Chl *a* m^{-2} d^{-1}, between December and February, with an overall mean of 25 mg Chl *a* m^{-2} d^{-1}. Taking 0.5 day^{-1} as reasonable value for phytoplankton growth rates in Antarctic waters [*Garzio et al.*, 2013], and using the mean summer time integrated Chl *a* value from Station B (55 mg m^{-2}; range 20 to 100), we derive a Chl *a* production term of 28 mg Chl *a* m^{-2} d^{-1}. The close match between the estimated Chl *a* production and grazing loss terms suggests a strong potential for top-down control of summertime phytoplankton biomass.

3.2. Seasonal Variability in Surface Water pCO_2 and $\Delta O_2/Ar$

Surface pCO_2 and $\Delta O_2/Ar$ were closely coupled with seasonal changes in phytoplankton biomass (Figure 1) and also influenced by higher frequency physical dynamics. We identified five phases characterizing the seasonal evolution of community metabolism. During the early season growth period (phase I), ice-covered surface waters exhibited pCO_2 supersaturation and negative $\Delta O_2/Ar$, indicative of remnant winter time net heterotrophy. The O_2 deficit was rapidly erased by net autotrophy, with pCO_2 and $\Delta O_2/Ar$ reaching atmospheric equilibrium within ~10 days. Phase II corresponded to the massive spring phytoplankton bloom and a remarkable accumulation of O_2 and pCO_2 drawdown in surface waters. Minimum pCO_2 at the height of the bloom was less than 50 μatm (~1930 μmol L^{-1} DIC), while a maximum $\Delta O_2/Ar$ of +70% was observed (~600 μmol kg^{-1} O_2). These biologically induced gas disequilibria are among the largest ever reported for a natural marine system. During the short-lived (~3 day) mixing event in early December, pCO_2 and $\Delta O_2/Ar$ exhibited a transient excursion toward atmospheric equilibrium. Approximately 2 weeks later, surface water pCO_2 and $\Delta O_2/Ar$ were rapidly reset to near equilibrium values, in conjunction with the crash of the phytoplankton bloom (phase III). Thereafter, $\Delta O_2/Ar$ and pCO_2 oscillated above and below air equilibrium during the extended midsummer period (phase IV), with a gradual decrease (increase) in $\Delta O_2/Ar$ (pCO_2). During the final few weeks of our sampling season (phase V), we observed consistent $\Delta O_2/Ar$ undersaturation and pCO_2 supersaturation, indicative of a return to net heterotrophic conditions.

3.3. Light-Driven Cycling of Surface pCO_2 and $\Delta O_2/Ar$

Superimposed on the large seasonal changes discussed above, surface water pCO_2 and $\Delta O_2/Ar$ exhibited pronounced diel oscillations associated with the daily cycles in surface irradiance. These diel cycles were present over the entire growth season but most apparent in the midsummer period (Figure 1, insets). Beginning shortly after dawn, we observed a rapid increase in $\Delta O_2/Ar$ (>10% change) and strong pCO_2 drawdown (>50 μatm), indicating excess photosynthesis over respiration in the water column (Figure 1, inset). Conversion of the ΔO_2 /Ar and pCO_2 data into O_2 and DIC concentrations, respectively, revealed a mean ratio of O_2 evolution to DIC production centered around 1:1 (Figure S2), consistent with expected biological stoichiometry [*Robinson et al.*, 1999]. Following this period of intense productivity, the water

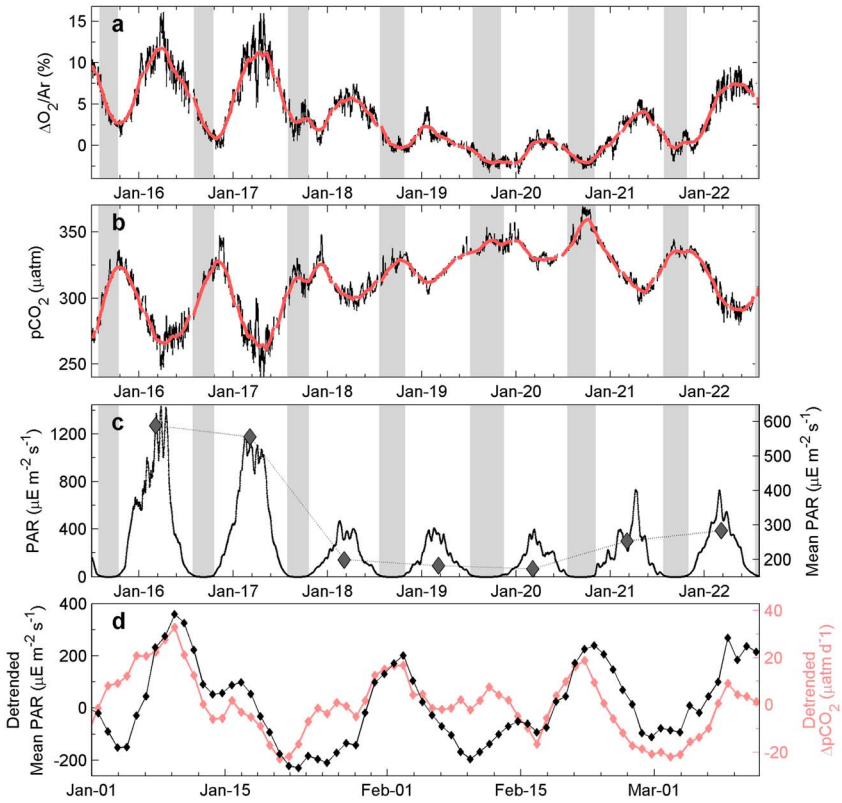

Figure 3. Influence of surface PAR variability on $\Delta O_2/Ar$ and pCO_2. (a–c) Diel cycles in $\Delta O_2/Ar$, pCO_2 and PAR over a 1 week period in mid-January. Diamonds in Figure 3c show daily average PAR levels. (d) Daily averages PAR and pCO_2 drawdown (daily maximum-minimum) during January–March. The daily average values were linearly detrended and smoothed using a three-point running mean filter.

column entered a net heterotrophic state by the midafternoon, with a strong decrease in $\Delta O_2/Ar$ (increase in pCO_2) indicative of excess community respiration. During the postbloom summer period, the negative (positive) slope in $\Delta O_2/Ar$ (pCO_2) was similar between the late afternoon and nighttime, suggesting that community respiration rates showed little diel periodicity. The daily shift from net autotrophy to net heterotrophy can thus be attributed to a decline in net photosynthesis rather than increased community respiration rates.

Diel oscillations in pCO_2 and $\Delta O_2/Ar$ were also observed during the spring phytoplankton bloom, although these cycles were partially obscured by the strong O_2 accumulation (pCO_2 drawdown) associated with net biomass increase. During the bloom, the net autotrophic period of each daily cycle dominated over the net heterotrophic phase, and the shift between these metabolic states occurred closer to the end of the daylight period (Figure 2). These observations are consistent with the recent results of J. Goldman et al. (Gross and net production during the spring bloom along the Western Antarctic Peninsula, submitted to *New Phytologist*, 2014), who measured low respiration in discrete bottle samples during the spring bloom period.

Previous results from Palmer Station [*Moline and Prezelin*, 1997] have demonstrated large (~twofold) diel changes in maximum biomass-normalized ^{14}C fixation capacity (P_{max}), resulting from variability in light harvesting capacity and/or from changes in RubisCO carboxylation rates [*Prezelin*, 1992]. During our study, we observed strong diel cycles in variable Chl *a* fluorescence (F_v/F_m; Figure 2), with strong midday decreases in F_v/F_m, followed by nighttime recovery indicative of down regulation and/or photoinhibition of functional PSII reaction centers. The extent to which this process may have influenced carbon fixation would depend upon potential changes in electron turnover rates through the remaining functional reaction centers [*Behrenfeld et al.*, 1998]. While our data do not allow us to directly address this question, our Fast Repetition Rate Fluorometry observations, in conjunction with the $\Delta O_2/Ar$ and pCO_2 data, provide compelling evidence for a diel rhythm in photosynthesis that is closely coupled with variability in surface irradiance on short (<hourly) time scales.

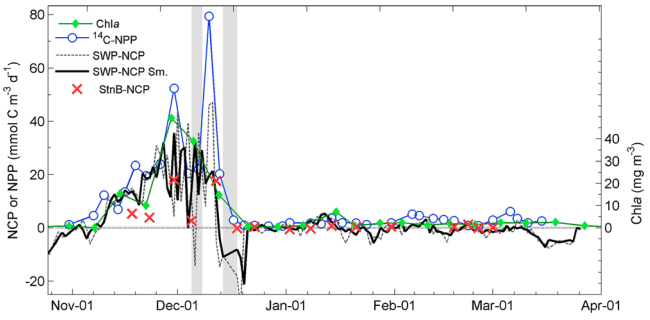

Figure 4. Daily net community production (NCP) derived from continuous $\Delta O_2/Ar$ measurements in the SWP supply and discrete mixed layer $\Delta O_2/Ar$ samples at PAL-LTER Station B. Chl *a* concentrations and ^{14}C-based net primary productivity (NPP) were measured in discrete samples from Station B. Vertical grey patches represent periods where physical mixing likely influenced the surface O_2 budget. O_2-based NCP was converted to carbon units using a photosynthetic quotient of 1 (see Figure S2).

Our results show that PAR variability on longer time scales (driven by regional meteorological forcing) also exerted a significant influence on surface water gas dynamics. Bright days with high mean PAR levels showed larger pCO_2 drawdown and O_2 accumulation than cloudy days with lower average PAR (Figure 3). The relationship between light intensity and biological gas cycling persisted over much of the midsummer growth period (January–March), during which we observed a strong coherence between daily pCO_2 drawdown and mean PAR levels (Figure 3d). The striking periodicity shown in Figure 3d results from the cyclical nature of storm systems along the WAP (Figure S3), which has been noted previously [*Moline and Prezelin*, 1997]. Taken together, our results highlight the importance of mixed layer irradiance as a controlling factor for summertime photosynthesis in near-shore WAP waters, and our high-resolution gas measurements provide a powerful observational tool to examine the influence of PAR variability over multiple time scales.

3.4. Metabolic Balance of Coastal WAP Waters

Our pCO_2 and $\Delta O_2/Ar$ data can be used to derive estimates of mixed layer NCP, using changes in surface gas concentrations as a measure of the net metabolic balance of the ecosystem. This approach is potentially complicated by physical disturbance of the mixed layer mass balance [*Kaiser et al.*, 2005] and by the possible influence of benthic processes on the SWP supply. During the 2012–2013 season, physical perturbations of the surface layer appeared to be limited to several short intervals in December, with strong density stratification acting to isolate the mixed layer during much of the summer (Figures 1c and 1d). The location of the SWP intake on a rocky bottom subject to glacial scouring and tidal flushing, acts to restrict sediment accumulation and algal colonization (C. Amsler, personal communication, 2013), thus minimizing the influence of benthic processes on the continuous seawater supply. These characteristics, combined with the shallow depth of the SWP intake (6 m), suggest that our measurements should reflect a mixed layer signal.

Our calculations show high-frequency NCP variability superimposed on a strong seasonal cycle (Figure 4). The early season, prebloom period was characterized by excess respiration (i.e., net heterotrophy), with computed NCP rates of ~ −7 mmol C m^{-3} d^{-1}. NCP became positive during early November, and this shift toward net autotrophy corresponded with the initial accumulation of phytoplankton biomass and an increase in ^{14}C-based net primary production rates (NPP). The period of net autotrophy lasted ~6 weeks, reaching a maximum NCP of ~30 mmol C m^{-3} d^{-1} in early December. High NCP during the phytoplankton bloom was punctuated by a brief excursion to negative NCP, likely resulting from a mixing event in early December (Figure 4). A second short-lived period of net heterotrophy (NCP ~ −20 mmol C m^{-3} d^{-1}) was observed during the crash of the phytoplankton bloom in late December. This negative NCP likely resulted from a combination of physical entrainment of low O_2 (high NO_3^-) waters and an increase in community respiration fueled by zooplankton grazing and enhanced bacterial production. Indeed, bacterial respiration rates (derived from PAL-LTER ^3H-Leucine incorporation data) exhibited a strong spike in mid-December to values of ~10 mmol C m^{-3} d^{-1}, contributing significantly to overall net O_2 consumption in the water column during the crash of the phytoplankton bloom. During the postbloom summer growth period, NCP remained close to zero, reflecting a tight coupling of photosynthesis and respiration over diel cycles. During the final phase of our seasonal sampling, NCP fell below zero, indicating a return to net heterotrophy.

Several lines of evidence suggest that our NCP estimates are quantitatively robust. Our values (maximum ~ 30 mmol m^{-3} d^{-1}) are well within the range of those reported in prior studies of coastal Antarctic phytoplankton [e.g., *Robinson et al.*, 1999]. Based on our MIMS data, we derive an integrated community production term of ~380 mmol C m^{-3} for phases I and II of the seasonal cycle (prior to the bloom crash). This

value is virtually identical to the computed mixed layer DIC drawdown at Station B (390 mmol C m^{-3}; derived from pCO_2 and alkalinity data) over this same interval. We also find good general agreement between our continuous NCP values and those obtained by Goldman et al. (submitted manuscript, 2014) from discrete analysis of ΔO_2/Ar samples at Station B during our field season (Figure 4). The discrete NCP values are based on a steady state mixed layer assumption, with the production signal integrated over the O_2 residence time in the mixed layer. As a result, these estimates cannot capture the high-frequency dynamics observed in our MIMS-based NCP values. Discrete NCP values, averaged over a ~1 week timescale, should be underestimates during periods of rapid biomass accumulation, while overestimation is expected during the bloom crash. Indeed, we observed this behavior in our comparison of discrete and continuous NCP estimates (Figure 4). In contrast, when the mixed layer was much closer to a steady state during the postbloom summer period, we observed excellent agreement between the discrete and continuous NCP values.

Our continuous MIMS-based NCP estimates also showed good coherence with net primary productivity estimates derived from standard 24 h ^{14}C incubations. Although direct comparison of NCP with ^{14}C-NPP is problematic [*Robinson et al.*, 1999], our NCP estimates were, on average, ~ 40–50% of ^{14}C-NPP (excluding one very high ^{14}C data point, and all negative NCP values). If ^{14}C-NPP measured over 24 h is assumed to represent gross primary production minus autotrophic respiration, our results imply that heterotrophic processes accounted for approximately half of the total community respiration. Results obtained from a variety of productivity methods (Goldman et al. submitted manuscript, 2014) indicate that the relative contribution of autotrophic and heterotrophic respiration likely changed significantly over the growth season, with low autotrophic respiration during the bloom phase. Although the coupling between NPP and NCP is likely subject to significant variability over time, the correspondence we observed between MIMS-based NCP values and ^{14}C NPP data provides confidence in our results as a reasonable productivity metric.

4. Concluding Remarks

High-frequency gas measurements provide a new observational window into the biological dynamics of coastal Antarctic waters, demonstrating metabolic responses to biological and physical forcing on various time scales. We observed one of the largest phytoplankton blooms ever recorded at Palmer Station, with unprecedented pCO_2 drawdown and O_2 accumulation. Although high rates of pCO_2 and O_2 cycling were observed across the full seasonal cycle, a tight coupling between autotrophic and heterotrophic processes constrained the net accumulation of carbon biomass in surface waters for much of the spring and summer. The annual spring bloom thus represents an exceptional period of net autotrophic metabolism, where photosynthesis exceeds respiration under conditions of high nutrient availability, peak solar irradiance, and low-grazing pressure. The crash of the phytoplankton bloom appeared to be driven by a combination of physical dynamics and zooplankton grazing, resulting in a short-lived, yet intense, period of net heterotrophy. During the extended postbloom summer period, zooplankton grazing likely exerted a dominant control on phytoplankton biomass, while mixed layer irradiance levels appeared to significantly influence daily production rates.

Despite physical perturbations of the mixed layer during some parts of the seasonal cycle, our continuous NCP estimates show good coherence with ^{14}C-derived NPP estimates. Incubation-based approaches are labor-intensive, and subject to containment artifacts [*Quay et al.*, 2010] and logistical constraints (e.g., weather-dependent sampling). By comparison, our method provides autonomous, high-resolution measurements which yield insight into surface water metabolic processes across a range of time scales. Future deployments of autonomous high-frequency gas measurement systems, in conjunction with ancillary sensors, could be used to monitor the response of high-latitude biogeochemical processes to on-going climate perturbations. On shorter time scales, high-resolution gas measurements, coupled with molecular and photophysiological analyses, could provide new insights into the adaptive metabolic strategies of plankton exposed to rapid environmental fluctuations in polar waters.

Acknowledgments

We wish to acknowledge the exceptional assistance provided by the science support and administrative staff at Palmer Station, and we also thank the entire Palmer LTER science team, Mike Stukel, in particular, for helpful discussions and assistance with micrograzing dilution experiments. This study was supported by funds from the U.S. National Science Foundation (OPP awards ANT-0823101, ANT-1043559, ANT-1043593, and ANT-1043532) as well as support for PDT and ECA from the National Science and Engineering Research Council of Canada. Data are freely available upon request.

The Editor thanks Peter Williams for his assistance in evaluating this paper.

References

Behrenfeld, M. J., O. Prasil, Z. S. Kolber, M. Babin, and P. G. Falkowski (1998), Compensatory changes in Photosystem II electron turnover rates protect photosynthesis from photoinhibition, *Photosynth. Res.*, *58*(3), 259–268.

Bernard, K. S., and D. K. Steinberg (2013), Krill biomass and aggregation structure in relation to tidal cycle in a penguin foraging region off the Western Antarctic Peninsula, *ICES J. Mar. Sci.*, *70*(4), 834–849.

Bernard, K. S., D. K. Steinberg, and O. M. E. Schofield (2012), Summertime grazing impact of the dominant macrozooplankton off the Western Antarctic Peninsula, *Deep Sea Res. Oceanogr. Res. Paper.*, *62*, 111–122.
Boyd, P. W. (2002), Environmental factors controlling phytoplankton processes in the Southern Ocean, *J. Phycol.*, *38*(5), 844–861.
Brewer, P. G., A. L. Bradshaw, and R. T. Williams (1986), Measurements of total carbon dioxide and alkalinity in the North Atlantic Ocean in 1981, in *The Changing Carbon Cycle*, pp. 348–370, Springer, New York.
Carrillo, C. J., R. C. Smith, and D. M. Karl (2004), Processes regulating oxygen and carbon dioxide in surface waters west of the Antarctic Peninsula, *Mar. Chem.*, *84*(3–4), 161–179.
Craig, H., and T. Hayward (1987), Oxygen supersaturation in the ocean—Biological versus physical contributions, *Science*, *235*(4785), 199–202.
Dickson, A. G., and F. J. Millero (1987), A comparison of the equilibrium constants for the dissociation of carbonic acid in seawater media, *Deep Sea Res. Oceanogr. Res. Paper.*, *34*(10), 1733–1743.
Ducklow, H. W. (2008), Long-term studies of the marine ecosystem along the west Antarctic Peninsula Preface, *Deep Sea Res. Topic. Stud. Oceanogr.*, *55*(18–19), 1945–1948.
Ducklow, H. W., and S. C. Doney (2013), What is the metabolic state of the oligotrophic ocean? A debate, *Ann. Rev. Mar. Sci.*, *5*, 525–533.
Ducklow, H. W., K. Baker, D. G. Martinson, L. B. Quetin, R. M. Ross, R. C. Smith, S. E. Stammerjohn, M. Vernet, and W. Fraser (2007), Marine pelagic ecosystems: The West Antarctic Peninsula, *Phil. Trans. Roy. Soc. Lond. Biol. Sci.*, *362*(1477), 67–94.
Emerson, S., P. D. Quay, C. Stump, D. Wilbur, and R. Schudlich (1995), Chemical tracers of productivity and respiration in the subtropical Pacific Ocean, *J. Geophys. Res.*, *100*(C8), 15,873–15,887, doi:10.1029/95JC01333.
Garzio, L. M., D. K. Steinberg, M. Erickson, and H. W. Ducklow (2013), Microzooplankton grazing along the Western Antarctic Peninsula, *Aquat. Microb. Ecol.*, *70*(3), 215–232.
Gorbunov, M. Y., Z. S. Kolber, and P. G. Falkowski (1999), Measuring photosynthetic parameters in individual algal cells by fast repetition rate fluorometry, *Photosynth. Res.*, *62*(2–3), 141–153.
Huang, K., H. Ducklow, M. Vernet, N. Cassar, and M. L. Bender (2012), Export production and its regulating factors in the West Antarctica Peninsula region of the Southern Ocean, *Global Biogeochem. Cycles*, *26*, GB2005, doi:10.1029/2010GB004028.
Kaiser, J., M. K. Reuer, B. Barnett, and M. L. Bender (2005), Marine productivity estimates from continuous O_2/Ar ratio measurements by membrane inlet mass spectrometry, *Geophys. Res. Lett.*, *32*, L19605, doi:10.1029/2005GL023459.
Knap, A. H., A. Michaels, A. R. Close, H. Ducklow, and Dickson, A. G. (1996), Protocols for the joint global ocean flux study (JGOFS) core measurements, *JGOFS, Reprint of the IOC Manuals and Guides No. 29, UNESCO 1994*, *19*.
Landry, M. R., J. Kirshtein, and J. Constantinou (1995), A refined dilution technique for measuring the community grazing impact of microzooplankton, with experimental tests in the Central Equatorial Pacific, *Mar. Ecol. Prog. Ser.*, *120*(1–3), 53–63.
Mehrbach, C., C. H. Culberson, J. E. Hawley, and R. M. Pytkowicz (1973), Measurement of apparent dissociation constants of carbonic acid in seawater at atmospheric pressure, *Limnol. Oceanogr.*, *18*(6), 897–907.
Moline, M. A., and B. B. Prezelin (1996), Long-term monitoring and analyses of physical factors regulating variability in coastal Antarctic phytoplankton biomass, in situ productivity and taxonomic composition over subseasonal, seasonal and interannual time scales, *Mar. Ecol. Prog. Ser.*, *145*(1–3), 143–160.
Moline, M. A., and B. B. Prezelin (1997), High resolution time-series data for 1991/1992 primary production and related parameters at a Palmer LTER coastal site: Implications for modeling carbon fixation in the Southern Ocean, *Polar Biol.*, *17*(1), 39–53.
Montes-Hugo, M., S. C. Doney, H. W. Ducklow, W. Fraser, D. Martinson, S. E. Stammerjohn, and O. Schofield (2009), Recent changes in phytoplankton communities associated with rapid regional climate change along the Western Antarctic Peninsula, *Science*, *323*(5920), 1470–1473.
Pierrot, D., et al. (2006), MS Excel program developed for CO_2 system calculations, ORNL/CDIAC-105. Carbon Dioxide Information Analysis Center, Oak Ridge National Laboratory, U. S. Department of Energy, Oak Ridge, Tenn.
Prezelin, B. B. (1992), Diel periodicity in phytoplankton production, *Hydrobiologia*, *238*, 1–35.
Prezelin, B. B., E. E. Hofmann, and M. A. Moline (2004), Physical forcing of phytoplankton community structure and primary production in continental shelf waters of the Western Antarctic Peninsula, *J. Mar. Res.*, *62*(3), 419–460.
Quay, P. D., C. Peacock, K. Björkman, and D. M. Karl (2010), Measuring primary production rates in the ocean: Enigmatic results between incubation and non-incubation methods at Station ALOHA, *Global Biogeochem. Cycles*, *24*, GB3014, doi:10.1029/2009GB003665.
Reuer, M. K., B. A. Barnett, M. L. Bender, P. G. Falkowski, and M. B. Hendricks (2007), New estimates of Southern Ocean biological production rates from O_2/Ar ratios and the triple isotope composition of O_2, *Deep Sea Res. Oceanogr. Res. Paper.*, *54*(6), 951–974.
Robinson, C., S. D. Archer, and P. J. L. Williams (1999), Microbial dynamics in coastal waters of East Antarctica: Plankton production and respiration, *Mar. Ecol. Prog. Ser.*, *180*, 23–36.
Smith, R. C., K. S. Baker, M. L. Byers, and S. E. Stammerjohna (1998), Primary productivity of the Palmer long term ecological research area and the Southern Ocean, *J. Mar. Syst.*, *17*(1), 245–259.
Smith, W. O., A. R. Shields, J. C. Dreyer, J. A. Peloquin, and V. Asper (2011), Interannual variability in vertical export in the Ross Sea: Magnitude, composition, and environmental correlates, *Deep Sea Res. Oceanogr. Res. Paper.*, *58*(2), 147–159.
Sweeney, C., D. A. Hansell, C. A. Carlson, L. A. Codispoti, L. I. Gordon, J. Marra, F. J. Millero, W. O. Smith, and T. Takahashi (2000), Biogeochemical regimes, net community production and carbon export in the Ross Sea, Antarctica, *Deep Sea Res. Topic. Stud. Oceanogr.*, *47*(15–16), 3369–3394.
Tortell, P. D. (2005), Dissolved gas measurements in oceanic waters made by membrane inlet mass spectrometry, *Limnol. Oceanogr. Meth.*, *3*, 24–37.
Tortell, P. D., C. Guéguen, M. C. Long, C. D. Payne, P. Lee, and G. R. DiTullio (2011), Spatial variability and temporal dynamics of surface water pCO_2, DO_2/Ar and dimethylsulfide in the Ross Sea, Antarctica, *Deep Sea Res. Oceanogr. Res. Paper.*, *58*(3), 241–259.
Wanninkhof, R. (1992), Relationship between wind-speed and gas exchange over the ocean, *J. Geophys. Res.*, *97*(C5), 7373–7382, doi:10.1029/92JC00188.
Williams, P. J. L., P. D. Quay, T. K. Westberry, and M. J. Behrenfeld (2013), The oligotrophic ocean is autotrophic, *Ann. Rev. Mar. Sci.*, *5*, 535–549.